Published in final edited form as:
Mol Cancer Res. 2008 March ; 6(3): 352–363.

Positive feedback between vascular endothelial growth factor-A and autotaxin in ovarian cancer cells

Malgorzata M. Ptaszynska, **Michael L. Pendrak**, **Russell W. Bandle**, **Mary L. Stracke***, and **David D. Roberts**
Laboratory of Pathology, Center for Cancer Research, National Cancer Institute, National Institutes of Health, NIH, Bethesda, MD 20892-1500

Abstract

Tumor cell migration, invasion, and angiogenesis are important determinants of tumor aggressiveness and these traits have been associated with the motility stimulating protein autotaxin (ATX). This protein is a member of the ecto-nucleotide pyrophosphatase and phosphodiesterase family of enzymes but unlike other members of this group, ATX possesses lysophospholipase D activity. This enzymatic activity hydrolyzes lysophosphatidylcholine (LPC) to generate the potent tumor growth factor and motogen, lysophosphatidic acid (LPA). In the current study, we demonstrate a link between ATX expression, LPA, and vascular endothelial growth factor (VEGF) signaling in ovarian cancer cell lines. Exogenous addition of VEGF-A to cultured cells induces ATX expression and secretion, resulting in increased extracellular LPA production. This elevated LPA, acting through LPA_4, modulates VEGF responsiveness by inducing VEGFR2 expression. Down-regulation of ATX secretion in SKOV3 cells using antisense morpholino oligomers significantly attenuates cell motility responses to VEGF, ATX, LPA, and LPC. These effects are accompanied by decreased LPA_4 and VEGFR2 expression as well as by increased release of soluble VEGFR1. Since LPA was previously shown to increase VEGF expression in ovarian cancer, our data suggest a positive feedback loop involving VEGF, ATX, and its product LPA that could affect tumor progression in ovarian cancer cells.

Introduction

Vascular endothelial growth factor-A (VEGF) is a potent stimulator of angiogenesis associated with physiological processes such as wound healing and the female reproductive cycle. In addition, its expression can be increased under pathological circumstances including ischemic diseases and tumor growth. Originally identified as an inducer of vascular permeability in endothelial cells, VEGF now has established roles in endothelial cell migration, proliferation, and survival. In cancer, VEGF exhibits autocrine activities that serve to protect tumor cells from stressors such as hypoxia, chemotherapy, or radiotherapy. Anti-VEGF treatments to limit these effects are in clinical use as well as in ongoing clinical trials (1,2).

VEGF signaling is mediated by two tyrosine kinase receptors, VEGFR1 (Flt-1) and VEGFR2 (KDR/Flk-1), both of which are crucial for VEGF-stimulated angiogenesis and are implicated in tumor progression. VEGF gene expression can be stimulated by low glucose levels, by growth factors such as fibroblast growth factor-2 (FGF2) or platelet-derived growth factor (PDGF), and in tumor cells, by alterations in oncogenic or tumor suppressor genes. However, the strongest inducer of VEGF expression is hypoxia, a common feature of the tumor microenvironment. In ovarian cancer, VEGF contributes to malignant ascites formation by

*Correspondence: Mary Stracke, Laboratory of Pathology, Center for Cancer Research, National Cancer Institute, National Institutes of Health, Bethesda, MD 20892-1500; TEL: 301-402-0044, FAX: 301-402-8911, email: stracke@helix.nih.gov.

increasing peritoneal micro-vessel permeability (3) and, interestingly, lysophosphatidic acid (LPA) in concentrations reported in malignant ascites has been found to induce VEGF expression (4,5). The bioactive lysophospholipid LPA stimulates cell proliferation, migration, and survival and has been implicated in tumor progression (6). Signaling of LPA is mediated through classic G protein-coupled receptors belonging to the endothelial differentiation gene (EDG) family (LPA_1/EDG-2, LPA_2/EDG-4, and LPA_3/EDG-7), and is linked to G proteins: $G_{q/11}$, $G_{i/o}$ and $G_{12/13}$. LPA_4 (GPR23/p2y9) is more closely related to purinergic P2Y than to EDG receptors and has distinct G protein-linked signaling: G_s, G_q, G_i, and $G_{12/13}$ (7,8). Under physiological circumstances, LPA concentrations in serum are approximately 1–10 μM. Although plasma concentrations are much lower (9), they can become elevated in cancer patients, particularly in ovarian cancer (10,11). The major source of serum and plasma LPA appears to be the lysophospholipase D activity of autotaxin (ATX, NPP2) (12,13).

ATX is a member of the ecto-nucleotide pyrophosphatase and phosphodiesterase family of enzymes and is synthesized as a secreted protein (14). In contrast to other members of this group, ATX possesses lysophospholipase D activity and can catalyze hydrolysis of lysophosphatidylcholine (LPC) into LPA and sphingosylphosphorylcholine into sphingosine-1-phosphate (15–17). ATX was initially purified as a potent chemotactic factor (18) and has been found to augment invasiveness and metastatic potential in transformed cells (19). These motogenic and invasive properties require its lysophospholipase D activity (19, 20). In addition, ATX stimulates angiogenesis (21) although the mechanisms for this action have not yet been elucidated.

In the present study we have focused on regulation of ATX expression in ovarian cancer cells and on the mechanisms by which it can contribute to ovarian cancer progression. Ovarian cancer ascites contains a number of bioactive molecules including VEGF, LPA, LPC, and sphingosylphosphorylcholine (22) and has elevated lysophospholipase D activity (23). We now present evidence that VEGF *via* VEGFR2 stimulates ATX expression in the ovarian cancer cell lines CaOV3 and SKOV3. In metastatic SKOV3 cells, treatment with a VEGF blocking antibody significantly decreases ATX mRNA levels, implying that the high level of ATX detected in this cell line is due to an autocrine action of VEGF. ATX knockdown *via* antisense morpholino oligomers (MO) results in reduced migration to VEGF, ATX, LPA and LPC. In addition, reduced ATX expression results in decreased LPA_4 and VEGFR2 signaling and release of the inhibitory soluble form of VEGFR1 (sVEGFR1), all of which may contribute to the decreased chemotactic response. These data indicate a regulatory role for VEGF in ATX synthesis as well as a role for ATX in controlling VEGF responsiveness. Since the ATX product LPA has been previously shown to increase VEGF expression (4,5), our data suggest a pathological positive feedback loop between ATX, LPA, and VEGF in ovarian carcinoma.

Results

Differential expression of VEGF and ATX in ovarian cancer cells

VEGF and LPA are major components of malignant ascites and their levels are associated with progression of ovarian carcinoma (24,25). Since ATX can generate extracellular LPA, which stimulates VEGF production in ovarian cancer cells, we looked for a correlation between ATX and VEGF expression in two ovarian cancer cell lines. SKOV3 cells were derived from an ovarian cancer malignant ascites, and CaOV3 were derived from a primary adenocarcinoma. Both are tumorigenic in mice, and SKOV3 have often been used in rodents to model malignant ascites formation (26).

Quantitative reverse transcriptase-polymerase chain reaction (RT-PCR) was used to establish baseline mRNA expression of ATX and VEGF in these cell lines. SKOV3 cells expressed ATX mRNA at levels 80-fold and VEGF mRNA at levels 40-fold higher than CaOV3 cells

(Fig. 1A). Both cell lines expressed similar levels of VEGFR1, VEGFR2, and the basal transcription component TAF9 (Fig. 1A). Thus, the two ovarian cancer cell lines differed in their basal expression of ATX and VEGF mRNA but expressed similar levels of VEGF receptors.

Consistent with the steady state mRNA levels, ATX protein could be easily detected by Western blot analysis in SKOV3 supernatants, but was near the limit of detection in CaOV3 cells (Fig. 1B, upper panel). However, when medium was analyzed from a greater number of cells, secreted ATX could also be detected in CaOV3 cells (Fig. 1B, lower panel). VEGF protein levels in conditioned media from each ovarian cancer cell line were determined by ELISA. Equal numbers of cells were seeded into 6 well dishes, and the culture media were harvested at 6, 12 and 24 h. Steady-state VEGF protein levels in SKOV3 were 10-fold higher than in CaOV3 cells (compare Fig. 1C and D, respectively). These data correlated with the higher VEGF mRNA levels detected in SKOV3 cells (Fig. 1A). Thus, under identical culture conditions, SKOV3 cells synthesized and secreted significantly more VEGF and ATX than CaOV3 cells.

Because LPA has been shown to stimulate VEGF expression in some ovarian cancer cells (4), both cell lines were treated with 20 μM LPA, and VEGF protein secreted into supernatants was assessed at 6, 12 and 24h. LPA treatment increased VEGF secretion in both cell lines (Fig. 1C and D). This increase was statistically significant only at the 12 h time point for SKOV3 cells (Fig.1C), possibly due to higher basal VEGF secretion in this cell line. In CaOV3 cells, significant induction of VEGF protein cells occurred at 12 and 24 h (Fig.1D). These data confirmed that extracellular LPA stimulates VEGF protein expression in these cells.

Migration responses of ovarian cancer cells

ATX-stimulated cellular motility requires hydrolysis of an appropriate substrate such as LPC to generate the chemotactic lysophospholipid LPA (20). To determine whether the differential ATX expression and secretion in these two ovarian cancer cell lines affected their motility responses, both cell lines were assayed side by side under identical conditions with 3 h incubations. This short time interval was chosen because it resulted in negligible background (random) migration (see Fig. 2, control values). Both cell lines displayed similar dose-dependent migration to recombinant $VEGF_{165}$ when compared to background (Fig. 2A). However, CaOV3 cells achieved maximal migration with 100 ng/ml VEGF while maximal migration of SKOV3 was shifted to a higher VEGF concentration (Fig. 2A). On the other hand, SKOV3 cells migrated better to ATX, its product LPA, and its substrate LPC (Fig. 2B, C, and D). There was no difference in migration to the enzymatically inactive ATX mutant, T210A-ATX, although migration was significantly above background for both cell lines (Fig. 2B).

VEGF stimulates ATX expression and secretion in ovarian cancer cells *via* VEGFR2

By generating exogenous LPA, ATX could contribute to the induction of VEGF in ovarian cancer cells (4). To determine whether VEGF also regulates ATX expression, cells were treated with recombinant $VEGF_{165}$ at concentrations that were previously established to induce a maximal migratory response (Fig.2A). After 16h incubation with VEGF, ATX mRNA levels were found to be increased up to 8-fold in SKOV3 cells (Fig. 3A) and up to 10-fold in CaOV3 cells (Fig. 3B). This increase was accompanied by a concomitant increase in secreted ATX protein as shown by immunoblot analysis of concentrated conditioned media from SKOV3 and CaOV3 cells (Fig. 3A and B,respectively). Therefore, despite the differential regulation of basal ATX expression in these two cell lines, ATX transcription in both could be further increased in response to exogenous VEGF.

If the higher basal VEGF level in SKOV3 cells was acting as an autocrine stimulus of ATX expression, then decreased VEGF could result in reduced ATX transcription. To address this question, SKOV3 cells were treated for 10 h with a monoclonal anti-VEGF antibody to neutralize endogenously secreted VEGF and ATX mRNA levels were then quantified. This treatment resulted in a dose-dependent decrease in ATX mRNA levels indicating an autocrine effect of secreted VEGF in this cell line (Fig. 3C). To determine whether signaling through VEGFR2 was required for this effect, SKOV3 cells were co-treated with VEGF and 25 nM of the VEGFR2 inhibitor V (ZM323881). This compound is specific for VEGFR2 (IC_{50} < 2 nM) compared to VEGFR1 (IC_{50} > 50μM) (27) and has been shown to inhibit signaling through MAPK, ERK and p38 when stimulated through VEGFR2, but not through receptors for epidermal growth factor (EGF), PDGF, or hepatocyte growth factor (28). In this experiment, VEGF treatment stimulated ATX mRNA expression approximately 3-fold over that in untreated cells, but ATX mRNA decreased about 5-fold when cells were co-treated with VEGFR2 inhibitor and VEGF (Fig. 3D).

The relationship between VEGF receptor signaling and ATX expression was further examined in low ATX-expressing CaOV3 cells. These cells were treated with agonistic antibodies to VEGFR1 and VEGFR2 for 10 h, after which ATX mRNA levels were measured. Treatment with the VEGFR2 agonist resulted in a significant increase in ATX mRNA levels while treatment with VEGFR1 agonistic antibody showed a lesser 2-fold increase that was not statistically significant (Fig. 3E). These results confirmed that VEGF signaling to the ATX promoter requires the participation of VEGFR2.

To investigate which VEGF receptor is the predominant mediator of the VEGF migratory response in these cells, SKOV3 cells were treated with antagonistic antibodies to VEGFR1 or VEGFR2 and VEGF-stimulated migration was then assayed. Addition of the VEGFR1 antagonist did not affect cell migration to VEGF (Fig. 3F); however, treatment with antibodies antagonistic to VEGFR2 significantly decreased this migration (Fig. 3G). Therefore, both stimulation of ATX gene expression by VEGF and migration to VEGF protein relied on VEGFR2 signaling in these ovarian cancer cell lines.

ATX expression in SKOV3 was transiently reduced after MO treatment

To reduce ATX protein expression and examine the effect of ATX levels on ovarian cancer cells, highly ATX-expressing SKOV3 cells were treated with ATX-specific morpholino oligomers (ATX-MO). Mismatched oligomers (MM-MO) were used as a specificity control. MDA-MB-435 (MDA-435) cells, which secrete high levels of ATX (29), served as positive controls for ATX expression and confirmed the efficacy of the knockdown.

SKOV3 cells were incubated for 24 or 48 h with morpholino oligomers followed by media replacement and an additional 15 h incubation in serum-free medium. This latter step was included to minimize contamination with any ATX present in serum. Treatment of SKOV3 cells with 5 – 10 μM ATX-MO decreased ATX expression by approximately 90% at both 24- and 48 h time points, whereas 10 μM MM-MO treatment had a negligible effect (Fig. 4A, upper panels). Similar results were seen in MDA-MB-435 cells except that 10 μM ATX-MO was required for a significant knockdown, consistent with the higher levels of ATX produced by these cells (Fig. 4A, lower panels). Cells treated with ATX-MO or MM-MO were assessed for viability by Trypan Blue exclusion and found to be essentially identical with respect to dye uptake (data not shown). These cells also appeared healthy by microscopic examination (Fig. 4B).

The inhibitory effects on ATX protein levels persisted up to 39 h after ATX-MO removal (Fig. 4C), but expression fully recovered by 63 h (data not shown). Thus, morpholino antisense oligomers could be used in SKOV3 cells to down-regulate ATX gene expression specifically

without noticeable effects on cell viability. Since this reduction in ATX expression persisted for at least 24 h after morpholino removal, the biological assays described below were performed within this time period.

Reduced ATX expression affected migration to LPC, ATX, LPA, and VEGF but not to epidermal growth factor (EGF)

ATX has been shown to stimulate cellular motility, invasiveness, angiogenesis, and experimental metastases in mice (19,21). Its stimulation of motility and invasion has been correlated to its lysophospholipase D activity (20) implying that reduction of ATX expression could limit the motility response to LPC. We tested this hypothesis in ATX-MO-treated SKOV3 cells.

As expected, ATX knockdown by ATX-MO resulted in a decreased motility response to the ATX substrate LPC. The specific motility responses (*i.e.*, minus background) induced by 50 μM LPC was reduced to about 5% of that of mock-transfected or MM-MO-treated cells (Fig. 5A). At an LPC concentration of 100 μM, ATX-MO-treated cells were partially able to overcome this effect (Fig. 5A). Migration increased to 41 – 47% of that seen in either control group, but inhibition remained statistically significant. These data imply that LPC-stimulated motility in SKOV3 cells is the result of ATX-catalyzed hydrolysis of LPC to LPA rather than a direct motility response to LPC. These results also confirmed an effective reduction in ATX expression by ATX-MO.

With LPA as chemoattractant, motility of ATX-MO treated cells was partially restored up to 50% of that seen in MM-MO control cells but remained significantly inhibited (Fig. 5A). Surprisingly, motility to VEGF was also significantly decreased in 10 h and 4 h migration assays (Fig. 5A and B). This suggested that the motility response of these cells to VEGF requires downstream activation or induction of ATX. Unexpectedly, the inhibition of specific motility in ATX-MO-treated cells was not overcome by adding external ATX (Fig. 5A).

To confirm that ATX knockdown was blocking a specific function of ATX rather than acting as a general inhibitor of motility, we tested the motility response of ATX-MO-treated SKOV3 cells to 30 ng/ml EGF. This EGF concentration produced maximal response in preliminary 5 h assays (data not shown). As shown in Fig. 5B, the cells retained their capacity to respond to EGF indicating that decreased ATX expression did not have a general inhibitory effect upon the locomotory capacity of the cells. Rather, inhibition was specific for the attractants LPA, LPC, ATX, and VEGF.

Reduction in ATX expression resulted in a significant decrease in LPA4 expression

Increased LPA production by ATX–catalyzed LPC hydrolysis is the established mechanism for ATX- based motility responses. Accordingly, one explanation for the decreased motility to ATX, LPA, and LPC seen after ATX-MO treatment could be that ATX knockdown induced changes in LPA receptor expression.

In order to test this hypothesis, we first determined steady state LPA receptor expression levels in CaOV3 and SKOV3 cells. Quantitative RT-PCR revealed that SKOV3 cells expressed higher LPA_1 and LPA_4 than CaOV3 cells (Fig. 5C). We next compared LPA receptor mRNA levels in MM-MO-treated vs. ATX-MO-treated SKOV3 cells. LPA_1 or LPA_2 expression did not change significantly after ATX-MO treatment (Fig. 5D). Although LPA_3 expression was reduced in dose-dependent manner after ATX knockdown this was not a statistically significant reduction. In contrast, LPA_4 expression was significantly reduced approximately 4-fold in a concentration-dependent manner (Fig. 5D)

Because the most profound decrease after ATX knockdown was observed in the expression of LPA_4, it seemed possible that ATX and its product, LPA, target this receptor. Therefore, we next determined whether LPA receptor expression could be regulated by extracellular LPA. Low ATX-expressing CaOV3 cells were treated with varying concentrations of LPA and the mRNA levels of all four LPA receptors were quantified. LPA_1 and LPA_2 expression were affected only by 10 μM LPA, which induced approximately 2-fold increases in both receptors (Fig. 5E). However, the mRNA levels of both LPA_3 and LPA_4 increased more than 10-fold in a concentration-dependent manner after treatment with 10 μM LPA (Fig. 5E). Taken together, these results suggest that increased ATX levels can modulate LPA-related cellular effects. More specifically, the resulting increase in the amount of extracellular LPA can differentially stimulate LPA_3 and LPA_4 expression.

Expression of VEGFR2 and sVEGFR1 in ATX knockdown cells

The decreased motility to VEGF in ATX knockdown cells could also be explained by altered expression of VEGF receptors. We examined this possibility utilizing RT-PCR to measure receptor mRNA levels in ATX-MO-treated SKOV3 cells. VEGFR2 expression decreased more than 5-fold after treatment with 10 μM ATX-MO (Fig. 6A). This receptor has been closely linked to the motility response induced by VEGF (Fig 3F and G) (30). VEGFR1 expression decreased approximately 2-fold after treatment with 10 μM ATX-MO, which was notably less than VEGFR2 (Fig. 6A). In contrast, the ATX knockdown had no significant effect on VEGF mRNA levels as detected by quantitative RT-PCR (Fig. 6A) or on the secreted VEGF protein levels as detected by ELISA (Fig. 6B).

The PCR primer pair used to detect VEGFR1 expression was specific for the membrane-anchored form of VEGFR1 rather than its alternatively spliced, soluble variant (sVEGFR1). Since sVEGFR1 can inhibit signaling through VEGFR2 by sequestering VEGF, we examined the effect of ATX knockdown on sVEGFR1 protein. Secreted VEGFR1 could be detected in cell culture supernatants from ATX-MO treated cells but not from controls (Fig. 6C).

Taken together, these data demonstrated that down-regulation of ATX expression limited the migratory response to VEGF, decreased expression of the major VEGF-responsive receptor (VEGFR2), and increased the release of VEGF-sequestering sVEGFR1.

VEGFR2 expression in ovarian cancer cells is stimulated by LPA and intracellular cAMP

The above data (Fig. 6) suggests that ATX protein levels modulate VEGF receptor expression. Several demonstrated effects of ATX are mediated through its product, LPA, including the ATX effect on LPA receptor expression (Fig. 5E). To determine whether LPA also mediates the ATX-induced changes in VEGF receptor expression, CaOV3 cells were treated with LPA at various concentrations then VEGF receptor mRNA levels were determined. VEGFR1 mRNA levels increased slightly, but VEGFR2 levels were more sensitive, increasing more than 4-fold after treatment with 10 μM LPA (Fig. 7A and B). These data indicate that LPA can stimulate both VEGF and VEGF receptor expression. Accordingly, an ATX knockdown would result in decreased extracellular LPA and could lead to changes in both VEGF receptor expression and VEGF signaling.

The ATX gene knockdown most profoundly affected LPA_4 expression, suggesting that the signaling cascade initiated by activation of this receptor could be involved in VEGF receptor regulation. LPA_4 is unique among the LPA receptors in that it utilizes the Gs pathway that activates protein kinase A (PKA) through cAMP. Thus, we tested whether VEGFR2 expression could be increased by the addition of exogenous cAMP. When dibutyryl-cAMP was added to SKOV3 cells, VEGFR2 mRNA levels increased more than 5-fold. Furthermore, VEGFR2 mRNA levels decreased in a time-dependent manner after treatment with the PKA inhibitor

Rp-MB-cAMPS (Fig.7C). This inhibitor is cleaved by intracellular esterases to release butyrate and Rp-cAMPS. The latter is a cAMP analogue that binds to PKA type I and type II, preventing holoenzyme dissociation and PKA activation. Interestingly, treatment with Rp-cAMPS resulted in a 4-fold increase in the mRNA levels of sVEGFR1 (Fig. 7D).

Taken together, this data revealed that activation of the LPA_4 Gs pathway, which increases intracellular cAMP and activates PKA, can regulate VEGFR2 expression and can consequently modulate VEGF signaling in these ovarian cancer cells.

Discussion

In ovarian cancer, VEGF has been shown to act as both an angiogenic factor that stimulates new blood vessel formation required for tumor survival (31), and as a potent vascular permeability factor involved in the formation of malignant ascites (3). However, there is growing evidence that VEGF plays additional roles in tumor progression. In tumor cells that express both VEGF and its receptors, VEGF acts in an autocrine manner to increase cell survival (32,33). Here, we report for the first time that VEGF stimulates the expression of ATX, a potent motility factor that is associated with the acceleration of cancer progression.

ATX generates the bioactive lysophospholipid LPA that regulates cell-cell interactions, inhibits apoptosis, and stimulates cellular migration and the production and action of extracellular proteases. Our data, combined with previous evidence that LPA increases VEGF expression in ovarian cancer cells (4,5), leads us to propose a positive feedback loop involving ATX, LPA, and VEGF and their cognate receptors (Fig. 8). This model proposes that feedback between VEGF and ATX occurs at more than one level. VEGF signaling *via* VEGFR2 stimulates both ATX mRNA expression and protein secretion. An increase in secreted ATX protein then increases the conversion of LPC to LPA, which in turn feeds back to increase expression of VEGF and VEGFR2 (Fig. 8). Through the production of this bioactive lysophospolipid, ATX positively regulates VEGFR2 expression and simultaneously limits the release of the inhibitory sVEGFR1 (Fig. 6). Thus, in ovarian carcinoma cells, this positive feedback pathway has the potential to simultaneously regulate tumor growth, angiogenesis, and metastatic spread.

Several lines of evidence validate this model. First, when the amount of endogenously produced VEGF available to SKOV3 cells was decreased utilizing an anti-VEGF antibody, ATX expression decreased in a dose-dependent manner (Fig. 3C). These results are consistent with an autocrine type signaling mechanism through VEGF receptors. Second, when signaling through VEGFR2 was blocked using a specific tyrosine kinase inhibitor of VEGFR2, ATX expression also decreased (Fig. 3D). Third, treatment with VEGFR2 agonistic antibody resulted in significant increase in ATX mRNA expression (Fig. 3E). Finally, addition of exogenous LPA could modulate the expression of both LPA and VEGF receptors (Fig. 5E and Fig. 7A). Taken together, these data indicate that limiting the ability of VEGF to signal through VEGFR2 limits ATX gene expression in these cells.

ATX gene knockdown experiments revealed another level of regulation involving cellular motility responses. After ATX reduction, SKOV3 cells exhibited a decrease in their migratory responses to specific chemotactic stimuli (LPC, LPA, ATX and VEGF), but not to EGF. An ATX knockdown would be expected to decrease the capacity of ATX to convert its substrate to its bioactive product, LPA. However, adding back either external ATX or LPA did not fully restore this reduced motility. Although our data revealed little effect of ATX knockdown on the expression of $LPA_{1–2}$, these decreased motility responses might be explained by the sensitivity of $LPA_{3–4}$ expression.

The receptor most profoundly affected by ATX knockdown was LPA_4. This receptor has low homology to the EDG family of LPA receptors and utilizes the Gs pathway to mediate an increase in intracellular cAMP, Gq/Gi to mediate release of intracellular calcium, and G12/13 to activate Rho (8). We showed that its expression could be induced by LPA (Fig. 5E) suggesting that a decrease in LPA concentrations after an ATX knockdown explains the decrease in LPA_4 expression and the decrease in signaling through this receptor. Because cAMP/PKA signaling (Fig. 7B–D) regulates VEGFR2 and sVEGFR1 mRNA levels in these cells, this pathway could account for the loss of migration to VEGR following ATX knockdown. Together, these data demonstrate that ATX expression modulates responsiveness to a specific subset of migratory stimuli, and the mechanisms may involve the ATX enzymatic product LPA and its associated signaling pathways.

VEGFR1 and VEGFR2 are specific genes that we found to be reduced by an ATX knockdown (Fig. 6A). VEGFR2 has a 10-fold lower affinity for VEGF though its tyrosine-kinase activity is 10–fold higher than VEGFR1. Our data indicates that VEGFR2 mediates both VEGF-stimulated migration and VEGF-induced up-regulation of ATX expression in the human ovarian cancer cell lines, CaOV3 and SKOV3. Others have found that VEGFR2 is important for initiation of angiogenesis (34) and migration in endothelial cells (30,35). Yang *et al*. demonstrated that activation of VEGFR2 in HUVECs was sufficient for VEGF-induced up-regulation of multiple genes, including growth factors, cytoskeletal-related proteins, chemokine receptors, signaling proteins, and transcription factors (36). This provides evidence that the reduction of VEGFR2 expression in ATX knockdown cells could affect a broad range of cellular processes.

Apart from the down-regulation of VEGFR2, the ATX gene knockdown also increased the release of the soluble form of VEGFR1 (sVEGFR1). This is a splice variant of VEGFR1 that lacks a tyrosine kinase and other domains but retains the high-affinity binding site for VEGF (37). Soluble VEGFR1 can sequester VEGF to reduce its availability to bind VEGFR2 (38) and can form an inactive heterodimer with VEGFR2 (39), thus acting as a negative regulator of VEGFR2 signaling. Therefore, ATX expression can directly or indirectly regulate at least two components involved in VEGF signal transduction.

Several growth factors, including EGF and FGF2, have been reported to increase ATX expression, while IL-1β, IL-4, and TGF-β decreased it in thyroid carcinoma cells (40). Another factor shown to increase ATX expression is α6β4. The α6β4 integrin is a laminin receptor that is typically associated with hemidesmosomes, which are stable adhesion complexes that contribute to the maintenance and organization of epithelial structures. However, in cancer cells, α6β4 can be up-regulated and lose its connection with hemidesmosomes, a change associated with a highly invasive phenotype (41). In the current manuscript, we have also found that up-regulation of ATX expression appears to be a component of a more motile phenotype. Previous work has associated ATX overexpression with increased invasiveness and metastases (19). Since loss of epithelial structure and induction of an invasive migratory phenotype are characteristic of metastatic carcinoma (42), it is interesting to speculate whether ATX expression might be associated with an epithelial-mesenchymal transition.

In the present work, we have shown that VEGF stimulates ATX expression, which in turn modulates VEGF responsiveness *via* its product LPA. These data imply cross-talk between these two proteins. VEGF plays a major role in tumor progression and ATX has been shown to increase invasiveness and metastatic potential (21). Although ATX is not an oncogene *per se*, it is an inducible enzyme and its expression can be modulated by external growth factors. We demonstrate here for the first time that induction of ATX expression by VEGF may be an important autocrine mechanism that participates in the generation of an aggressive phenotype in ovarian cancer and accelerates cancer progression. As a secreted protein, ATX may prove

to be a beneficial target for cancer therapy, one that decreases both LPA production and signaling and VEGF signaling.

Materials and Methods

Reagents

All chemicals were reagent grade and were obtained from Sigma-Aldrich (St. Louis, MO) unless otherwise noted. Stock solutions for oleoyl-La-lysophosphatidic acid sodium salt (LPA) were prepared in distilled, deionized water and for 1-Oleoyl-snglycero-3 phosphocholine (LPC) were prepared in ethanol. Human recombinant epidermal growth factor (EGF), human collagen type IV, and $VEGFA_{165}$ (VEGF) were purchased from Bioscience (Gaithersburg, MD). VEGFR2 kinase inhibitor V (ZM323881), Adenosine3',5'-cyclic Monophosphorothioate,2'-O-Monobutyryl-,Rp- Isomer, Sodium Salt (Rp-cAMPS), and dibutyryl cAMP were obtained from Calbiochem - EMD Biosciences (Madison, WI). ATX was isolated from High Five insect cells as described previously (17). Antibodies were used at the concentrations suggested by the manufacture and concentrations used in these studies are indicated in figure descriptions. Anti-human VEGFR1 antibody (polyclonal rabbit, catalog # NB100-527SS) and anti-VEGF antibody (mouse monoclonal, catalog # NB100-564SS) were from Novus Biologicals Inc. (Littleton, CO). Agonistic antibody of human VEGFR1 (mouse monoclonal, mv1004m-h), agonistic antibody of human VEGFR2 (mouse monoclonal, mv1001.3m-h), antagonistic antibody of human VEGFR2 (mouse monoclonal, mv1001.1m-h), and antagonistic antibody of human VEGFR1 (rabbit polyclonal, pV1004R-h) were purchased from Angio-Proteomie (Boston, MA). The human VEGF ELISA detection kit was obtained from (R&D Systems, Minneapolis, MN).

Cell Culture

The human ovarian cancer cell lines SKOV3 (HTB-77) and CaOV3 (HTB-75) were obtained from ATCC (Manassas, VA), and the human breast cancer cell line MDAMB-435 was provided by Dr Patricia Steeg (CCR, NIH, Bethesda, MD) These cell lines were maintained in Dulbecco's Modified Eagle's Medium (DMEM from Biofluids, Rockville, MD) supplemented with 10% v/v heat-inactivated fetal bovine serum (Biosource, Camarillo, CA) and cultured at 37°C in a 5% CO_2 atmosphere.

Gene Knockdown

Knockdown of the ATX gene utilized antisense morpholino phosphorodiamidate oligomers constructed by GeneTools (Philomath, OR). The ATX-specific morpholino oligomer construct (ATX-MO) spanned the second splice site junction of the ATX gene (NM_006209, coordinates 406–407) and contained the sequence AGT TTT GAC ACT TAC CTG TAG GAG G. A control morpholino oligomer containing a 5-base mismatch (MM-MO) had the sequence ACT TTT CAC ACT TAG CTG TAC GAC G. Transfections were carried out with Endo-Porter (GeneTools) under conditions optimized according to the protocol suggested by the company. Cells were seeded into duplicate T - 75 flasks at 10^6 cells per flask and treated with 5 – 10 μM ATX-MO for 48 h. Negative controls included cells from the same passage identically transfected with MM-MO as well as cells treated with Endo-Porter alone (mock control).

For each experiment, removal of the transfection reagents was followed by a brief rinse with PBS then incubation in fresh DMEM without serum for 12 – 15 h. Cells maintained for 4 – 6 days were cultured with oligomers for 48 h, rinsed and kept in complete medium until changing to serum-free medium 15 h before the planned time point. Supernatants were collected and concentrated approximately 40-fold using an Amicon-Ultra-4 Centrifugal Filter Device (Millipore, Bedford, MA) with 10,000 MWCO. The remaining cells were harvested and utilized for RNA isolation, motility assays, or protein extraction.

Protein was extracted from whole cells in 1X ice-cold magnesium lysis buffer (MLB, Upstate, Charlottesville, VA) using instructions provided by the manufacturer.

Quantitative RT-PCR analysis

Total RNA was isolated utilizing Trizol™ per the manufacturer's instructions (Invitrogen) and reverse transcribed using oligo-dT primers with 5 μg total RNA and Superscript III reverse transcriptase. Quantitative PCR utilized 4.5% of total cDNA product and was amplified using Platinum SYBR Green qPCR SuperMix UDG (Invitrogen) for 40 cycles. Fluorescent intensity data were measured on an Opticon I instrument and processed with Opticon I software (Bio-Rad Laboratories, Hercules, CA). Melting curve analysis was performed for each sample to insure a single product was produced in each reaction. Oligonucleotide primers were designed using Fast PCR software (http://www.biocenter.helsinki.fi/bi/Programs/fastpcr.htm): for ATX (ENPP2, NM_006209): CTTTCGGCCCTGAGGAGAGTA and AGCAACTGGTCTTTCCTGTCT; for hypoxanthine phosphoribosyltransferase 1 (HPRT1, NM_000194): ATTGTAATGACCAGTCAACAGGG and GCATTGTTTTGCCAGTGTCAA; for TATA box binding protein associated factor (TAF9, NM_003187): ACTCCCACACTAGGCACAC and TGAGAAGTAGGCATCTGTACTGT; for VEGFR1: TGGCTGCGACTCTCTTCTG, and CAAAGGAACTTCATCTGGGTCC; for soluble VEGFR1: ACAGCCTTTTTGTTGCAGTGC and TTCAGGCACCTATGCCTGCAC (designed with FastPCR, http://www.biocenter.helsinki.fi/bi/programs/fastpcr.htm); for VEGFR2: TGGGGGAGCGTGTCAGAAT and CCGCTTTAATTGTGTGATTGGAC; for VEGF: GCGGATCAAACCTCACCAAG and GCTTTCGTTTTTGCCCCTTTC. Primers for LPA receptors have been previously described (43).

Immunoblot analysis

Conditioned media were collected and concentrated as described above. Samples were prepared for immunoblot analysis in LDS Sample Buffer (Invitrogen, Carlsbad, CA) containing 2% β–mercaptoethanol, heated to 95°C for 5 min and stored at −20 °C. Prior to gel loading, samples of 20 μg total protein were heated to 70°C. Electrophoresis was carried out using 10% NuPage Gels and NuPage MOPS running buffer and transferred on PVDF membranes (0.45μm pores) in Transfer Buffer (Invitrogen). ATX was detected using an anti-peptide antibody generated in rabbits as previously described (17). For VEGFR1 detection, whole cell lysates were prepared as described above and diluted in LDS sample buffer with 2% β-mercaptoethanol. Anti-VEGFR1 antibody (1:200) was from Santa Cruz Biotechnology (Santa Cruz, CA) and anti-sVEGFR1 (1:100) was from Novus Biologicals (Littleton, CT).

Motility assays

Migration was performed in 48-well modified Boyden chambers (Neuroprobe, Cabin John, MD) as described previously (44) but with the following modifications. Upper and lower chambers were separated by 8-μm pore size polycarbonate filters (Nucleopore) that had been pre-coated with human collagen type IV at 50 μg/ml in 0.1 M acetic acid. Cells were incubated for 3–4 h or as indicated in the figure legend under standard culture conditions after which the membranes were fixed and stained as described previously (21). Assays were performed in duplicate and quantified by counting three randomly chosen fields under light microscopy. All figures are representative of two or more independent experiments.

Treatment with antagonistic human VEGFR1 and VEGFR2 antibodies

Cells were pretreated with antibody for 15 minutes and antibody was present during migration assays. After 3 h incubation the migration assay was developed as described above and the number of migrated cells was determined by counting 3 –5 random fields.

To establish ATX mRNA levels after treatment with antibodies, cells were seeded in 6 well dishes at 200 000 per well and cultured overnight using basic culture conditions. Then, the cells were washed and antibody was added at concentrations suggested by the producer. After 10 h incubation, RNA was isolated as described above.

Human VEGF immunoassay (ELISA)

Cells were seeded in 6-well dishes at 200 000 per well and were cultured overnight in normal cultured conditions, then the medium was removed and cells were starved for an additional 12 h in serum free medium containing 0.01% BSA. This medium was removed and either fresh serum-free medium or 20 μM of LPA was added to the cells. Supernatant collection was performed at 6, 12 and 24 h. VEGF-A protein was measured according to the protocol provided by the company.

Statistical Analysis

Results of motility assays and quantitative RT-PCR were compared with Prism 4.0 software (GraphPad Software, San Diego, CA), utilizing one-way ANOVA with Tukey's post-test.

Acknowledgements

We wish to thank Elliott Schiffmann and Timothy Clair for their helpful advice in preparing the manuscript. This research was supported by the Intramural Research Program of the Center for Cancer Research, National Cancer Institute, National Institutes of Health.

References

1. Byrne AM, Bouchier-Hayes DJ, Harmey JH. Angiogenic and cell survival functions of vascular endothelial growth factor (VEGF). J Cell Mol Med 2005;9:777–794. [PubMed: 16364190]
2. Panares RL, Garcia AA. Bevacizumab in the management of solid tumors. Expert Rev Anticancer Ther 2007;7:433–435. [PubMed: 17428164]
3. Nagy JA, Masse EM, Herzberg KT, et al. Pathogenesis of ascites tumor growth: vascular permeability factor, vascular hyperpermeability, and ascites fluid accumulation. Cancer Res 1995;55:360–368. [PubMed: 7812969]
4. Hu YL, Tee MK, Goetzl EJ, et al. Lysophosphatidic acid induction of vascular endothelial growth factor expression in human ovarian cancer cells. J Natl Cancer Inst 2001;93:762–768. [PubMed: 11353786]
5. Lee J, Park SY, Lee EK, et al. Activation of hypoxia-inducible factor-1alpha is necessary for lysophosphatidic acid-induced vascular endothelial growth factor expression. Clin Cancer Res 2006;12:6351–6358. [PubMed: 17085645]
6. Ren J, Xiao YJ, Singh LS, et al. Lysophosphatidic acid is constitutively produced by human peritoneal mesothelial cells and enhances adhesion, migration, and invasion of ovarian cancer cells. Cancer Res 2006;66:3006–3014. [PubMed: 16540649]
7. Noguchi K, Ishii S, Shimizu T. Identification of p2y9/GPR23 as a novel G protein-coupled receptor for lysophosphatidic acid, structurally distant from the Edg family. J Biol Chem 2003;278:25600–25606. [PubMed: 12724320]
8. Lee C-W, Rivera R, Dubin AE, Chun J. LPA4/GPR23 Is a Lysophosphatidic Acid (LPA) Receptor Utilizing Gs-, Gq/Gi-mediated Calcium Signaling and G12/13-mediated Rho Activation. J Biol Chem 2007;282:4310–4317. [PubMed: 17166850]
9. Aoki J. Mechanisms of lysophosphatidic acid production. Semin Cell Dev Biol 2004;15:477–489. [PubMed: 15271293]
10. Xu Y, Shen Z, Wiper DW, et al. Lysophosphatidic acid as a potential biomarker for ovarian and other gynecologic cancers. Jama 1998;280:719–723. [PubMed: 9728644]
11. Mills GB, Fang X, Lu Y, et al. Specific keynote: molecular therapeutics in ovarian cancer. Gynecol Oncol 2003;88:S88–S92. [PubMed: 12586094]discussion S3-6

12. Tanaka M, Okudaira S, Kishi Y, et al. Autotaxin stabilizes blood vessels and is required for embryonic vasculature by producing lysophosphatidic Acid. J Biol Chem 2006;281:25822–25830. [PubMed: 16829511]

13. van Meeteren LA, Ruurs P, Stortelers C, et al. Autotaxin, a secreted lysophospholipase D, is essential for blood vessel formation during development. Mol Cell Biol 2006;26:5015–5022. [PubMed: 16782887]

14. Jansen S, Stefan C, Creemers JW, et al. Proteolytic maturation and activation of autotaxin (NPP2), a secreted metastasis-enhancing lysophospholipase D. J Cell Sci 2005;118:3081–3089. [PubMed: 15985467]

15. Umezu-Goto M, Kishi Y, Taira A. Autotaxin has lysophospholipase D activity leading to tumor cell growth and motility by lysophosphatidic acid production. J Cell Biol 2002;158:227–233. [PubMed: 12119361]

16. Tokumura A, Majima E, Kariya Y, et al. Identification of human plasma lysophospholipase D, a lysophosphatidic acid-producing enzyme, as autotaxin, a multifunctional phosphodiesterase. J Biol Chem 2002;277:39436–39442. [PubMed: 12176993]

17. Clair T, Aoki J, Koh E, et al. Autotaxin hydrolyzes sphingosylphosphorylcholine to produce the regulator of migration, sphingosine-1-phosphate. Cancer Res 2003;63:5446–5453. [PubMed: 14500380]

18. Stracke ML, Krutzsch HC, Unsworth EJ, et al. Identification, purification, and partial sequence analysis of autotaxin, a novel motility-stimulating protein. J Biol Chem 1992;267:2524–2529. [PubMed: 1733949]

19. Nam SW, Clair T, Campo CK, Lee HY, Liotta LA, Stracke ML. Autotaxin (ATX), a potent tumor motogen, augments invasive and metastatic potential of ras-transformed cells. Oncogene 2000;19:241–247. [PubMed: 10645002]

20. Koh E, Clair T, Woodhouse EC, Schiffmann E, Liotta L, Stracke M. Site-directed mutations in the tumor-associated cytokine, autotaxin, eliminate nucleotide phosphodiesterase, lysophospholipase D, and motogenic activities. Cancer Res 2003;63:2042–2045. [PubMed: 12727817]

21. Nam SW, Clair T, Kim YS, et al. Autotaxin (NPP-2), a metastasis-enhancing motogen, is an angiogenic factor. Cancer Res 2001;61:6938–6944. [PubMed: 11559573]

22. Yeo KT, Wang HH, Nagy JA, et al. Vascular permeability factor (vascular endothelial growth factor) in guinea pig and human tumor and inflammatory effusions. Cancer Res 1993;53:2912–2918. [PubMed: 8504432]

23. Tokumura A, Kume T, Fukuzawa K, et al. Peritoneal fluids from patients with certain gynecologic tumor contain elevated levels of bioactive lysophospholipase D activity. Life Sci 2007;80:1641–1649. [PubMed: 17367815]

24. Yamamoto S, Konishi I, Mandai M, et al. Expression of vascular endothelial growth factor (VEGF) in epithelial ovarian neoplasms: correlation with clinicopathology and patient survival, and analysis of serum VEGF levels. Br J Cancer 1997;76:1221–1227. [PubMed: 9365173]

25. Mills GB, Eder A, Fang X, et al. Critical role of lysophospholipids in the pathophysiology, diagnosis, and management of ovarian cancer. Cancer Treat Res 2002;107:259–283. [PubMed: 11775454]

26. Yu D, Wolf JK, Scanlon M, Price JE, Hung MC. Enhanced c-erbB-2/neu expression in human ovarian cancer cells correlates with more severe malignancy that can be suppressed by E1A. Cancer Res 1993;53:891–898. [PubMed: 8094034]

27. Whittles CE, Pocock TM, Wedge SR, et al. ZM323881, a novel inhibitor of vascular endothelial growth factor-receptor-2 tyrosine kinase activity. Microcirculation 2002;9:513–522. [PubMed: 12483548]

28. Endo A, Fukuhara S, Masuda M, Ohmori T, Mochizuki N. Selective inhibition of vascular endothelial growth factor receptor-2 (VEGFR-2) identifies a central role for VEGFR-2 in human aortic endothelial cell responses to VEGF. J Recept Signal Transduct Res 2003;23:239–254. [PubMed: 14626450]

29. Yang SY, Lee J, Park CG, et al. Expression of autotaxin (NPP-2) is closely linked to invasiveness of breast cancer cells. Clin Exp Metastasis 2002;19:603–608. [PubMed: 12498389]

30. Rousseau S, Houle F, Kotanides H, et al. Vascular endothelial growth factor (VEGF)-driven actin-based motility is mediated by VEGFR2 and requires concerted activation of stress-activated protein

kinase 2 (SAPK2/p38) and geldanamycin-sensitive phosphorylation of focal adhesion kinase. J Biol Chem 2000;275:10661–10672. [PubMed: 10744763]

31. Carmeliet P. VEGF as a key mediator of angiogenesis in cancer. Oncology 2005;69:4–10. [PubMed: 16301830]
32. Pidgeon GP, Barr MP, H HJ, Foley DA, Bouchier-Hayes DJ. Vascular endothelial growth factor (VEGF) upregulates BCL-2 and inhibits apoptosis in human and murine mammary adenocarcinoma cells. Br. J. Cancer 2001;85:273–278. [PubMed: 11461089]
33. Lee TH, Seng S, Sekine M, et al. Vascular Endothelial Growth Factor Mediates Intracrine Survival in Human Breast Carcinoma Cells through Internally Expressed VEGFR1/FLT1. PLoS Med 2007;4:e186. [PubMed: 17550303]
34. Shibuya M. Differential roles of vascular endothelial growth factor receptor-1 and receptor-2 in angiogenesis. J Biochem Mol Biol 2006;39:469–478. [PubMed: 17002866]
35. Gille H, Kowalski J, Li B, et al. Analysis of biological effects and signaling properties of Flt-1 (VEGFR-1) and KDR (VEGFR-2). A reassessment using novel receptor-specific vascular endothelial growth factor mutants. J Biol Chem 2001;276:3222–3230. [PubMed: 11058584]
36. Yang S, Toy K, Ingle G, et al. Vascular endothelial growth factor-induced genes in human umbilical vein endothelial cells: relative roles of KDR and Flt-1 receptors. Arterioscler Thromb Vasc Biol 2002;22:1797–1803. [PubMed: 12426207]
37. Hasumi Y, Mizukami H, Urabe M, et al. Soluble FLT-1 expression suppresses carcinomatous ascites in nude mice bearing ovarian cancer. Cancer Res 2002;62:2019–2023. [PubMed: 11929819]
38. Kendall RL, Thomas KA. Inhibition of vascular endothelial cell growth factor activity by an endogenously encoded soluble receptor. Proc Natl Acad Sci U S A 1993;90:10705–10709. [PubMed: 8248162]
39. Kendall RL, Wang G, Thomas KA. Identification of a natural soluble form of the vascular endothelial growth factor receptor, FLT-1, and its heterodimerization with KDR. Biochem Biophys Res Commun 1996;226:324–328. [PubMed: 8806634]
40. Kehlen A, Lauterbach R, Santos AN, et al. IL-1 beta- and IL-4-induced down-regulation of autotaxin mRNA and PC-1 in fibroblast-like synoviocytes of patients with rheumatoid arthritis (RA). Clin Exp Immunol 2001;123:147–154. [PubMed: 11168012]
41. Rabinovitz I, Toker A, Mercurio AM. Protein kinase C-dependent mobilization of the alpha6beta4 integrin from hemidesmosomes and its association with actin-rich cell protrusions drive the chemotactic migration of carcinoma cells. J Cell Biol 1999;146:1147–1160. [PubMed: 10477766]
42. Bagnato A, Rosano L. Epithelial-mesenchymal transition in ovarian cancer progression: a crucial role for the endothelin axis. Cells Tissues Organs 2007;185:85–94. [PubMed: 17587812]
43. Hama K, Aoki J, Fukaya M, et al. Lysophosphatidic acid and autotaxin stimulate cell motility of neoplastic and non-neoplastic cells through LPA1. J Biol Chem 2004;279:17634–17639. [PubMed: 14744855]
44. Aznavoorian S, Stracke ML, Parsons J, McClanahan J, Liotta LA. Integrin alphavbeta3 mediates chemotactic and haptotactic motility in human melanoma cells through different signaling pathways. J Biol Chem 1996;271:3247–3254. [PubMed: 8621727]

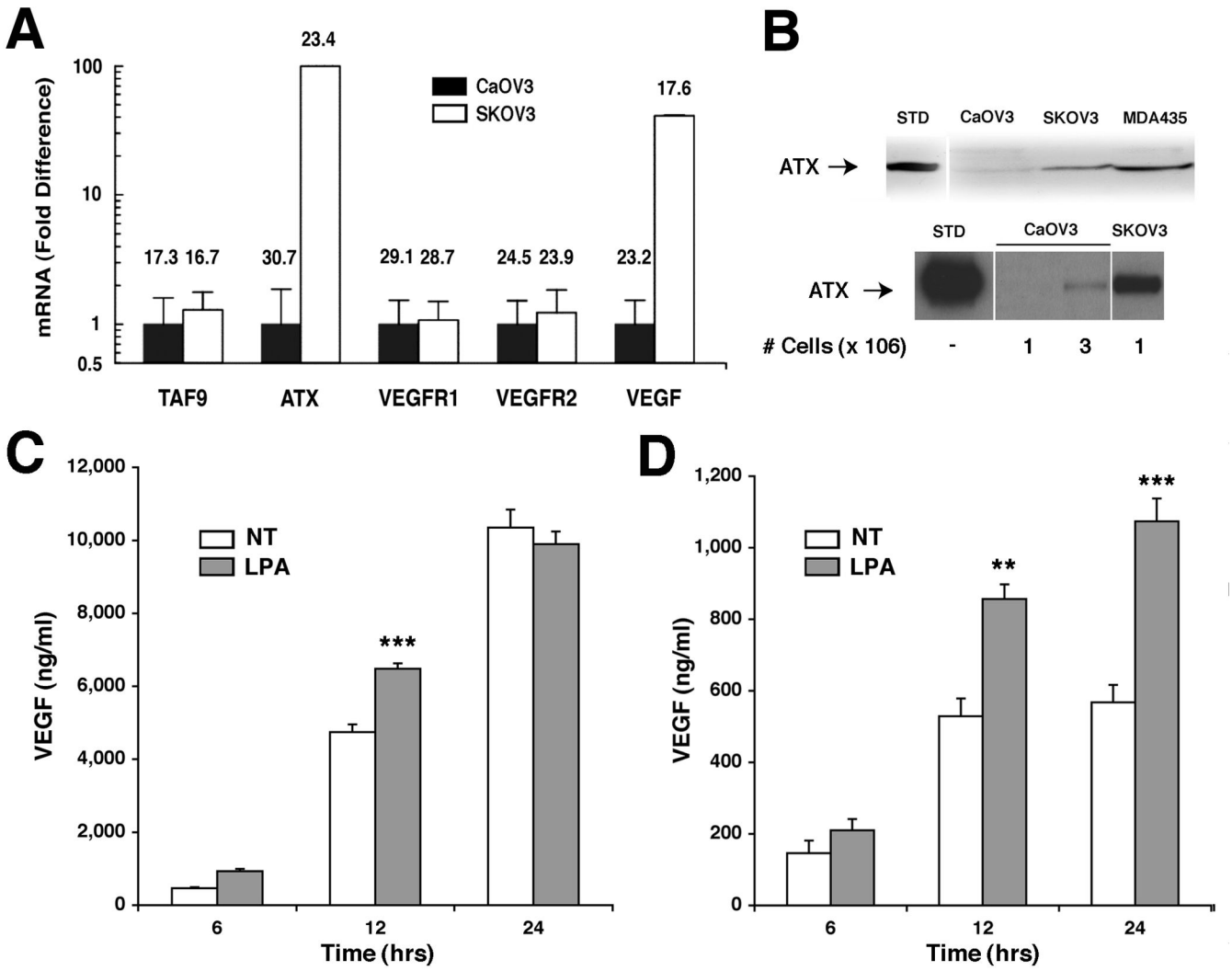

Figure 1. ATX and VEGF expression and motility stimulation in ovarian carcinoma cell lines

(**A**) Quantitative RT-PCR analysis of mRNA expression in SKOV3 and CaOV3 cells. Fold-expression for each gene set was adjusted to *HPRT1* internal control values and then expressed relative to CaOV3 levels, arbitrarily set to 1.0. C_T values for each data point are shown above each bar. *TAF9* expression was included as an additional internal control. (**B**) Immunoblot analyses of ATX protein in concentrated supernatants from SKOV3, CaOV3, or MDA-MB-435 cells are shown after a 12 h incubation with 10^6 cells (upper blot) or cell number as indicated (lower blot). (**C** and **D**) VEGF protein levels in SKOV3 (**C**) or CaOV3 (**D**) cell supernatants as measured by ELISA after the indicated times in culture with or without 20μM LPA; NT indicates non-treated controls. Results are shown as average ± SD; statistical comparisons are: *** for $P < 0.001$, ** for $P < 0.01$.

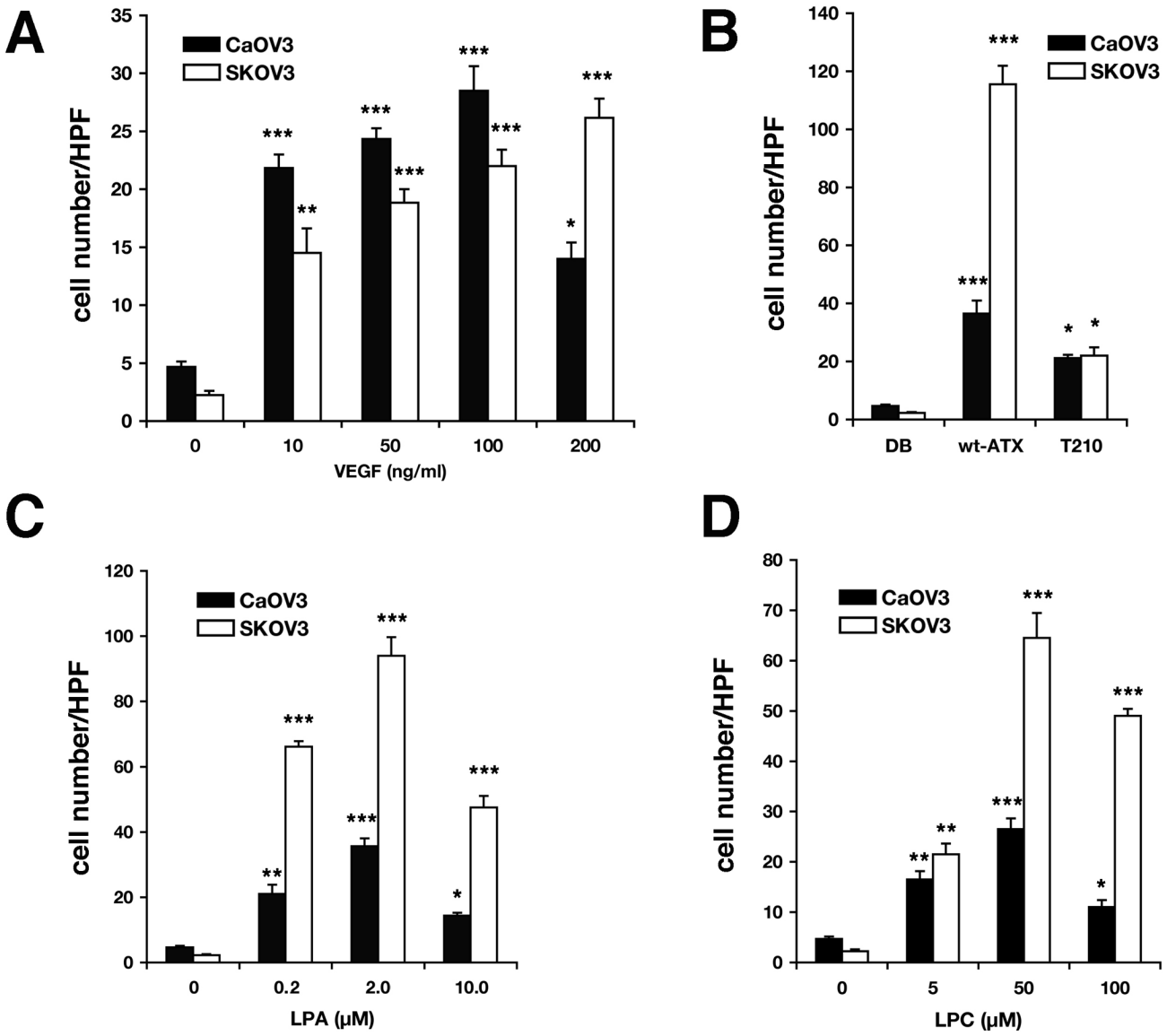

Figure 2. Migration of Ovarian Cancer Cells to ATX, VEGF, LPC and LPA

SKOV3 and CaOV3 cells were tested side-by-side in a modified Boyden chamber assay. Migration after a 3 h incubation to (**A**) VEGFA165 at indicated concentrations, (**B**) recombinant wild type ATX and a catalytically inactive form (T210A-ATX) at 2.4 nM, (**C**) LPA and (**D**) LPC at indicated concentrations. Results are shown as the average number of cells per high power field (HPF) ± SD. Statistical comparisons to the appropriate baseline motility (no attractant) are shown: *** for $P < 0.001$; ** for $P < 0.01$; * for $P < 0.05$.

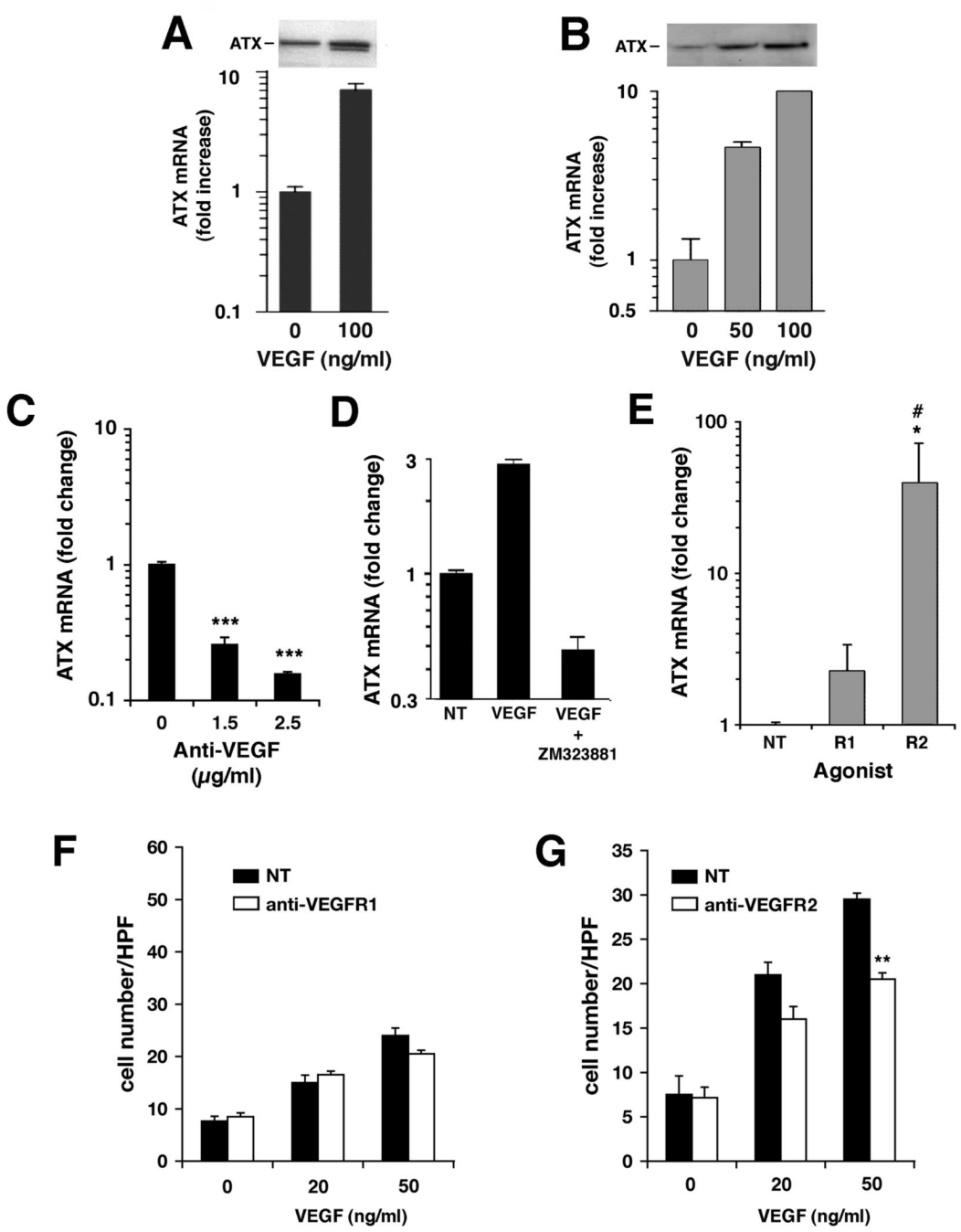

Figure 3. VEGF signaling to the ATX promoter is a VEGFR2-dependent process

(**A**) SKOV3 (solid black bars) or (**B**) CaOV3 (gray bars) cells were treated for 16 h with indicated concentrations of $VEGFA_{165}$ and assayed for ATX steady-state mRNA levels by quantitative RT-PCR (graph), or for secreted ATX protein levels by Western analysis (inset). (**C**) SKOV3 cells were cultured in the presence or absence of a VEGF-specific blocking antibody for 10 h at the indicated concentrations, and analyzed for ATX steady-state mRNA levels by quantitative RT-PCR. (**D**) SKOV3 cells were concurrently treated with 25 nM VEGFR2 inhibitor (ZM323881) and 100 ng/ml VEGF for 10 h and analyzed for ATX mRNA levels as described in (A). (**E**) CaOV3 cells were treated with VEGF receptor agonist antibodies specific for VEGFR1 or VEGFR2 (at 25 μg/ml and 5 μg/ml, respectively). ATX transcription

was measured as described in (A). (**F** and **G**) SKOV3 cell motility was measured in modified Boyden chambers in the presence of $VEGFA_{165}$ at the indicated concentrations. Cells were pre-incubated with VEGF receptor antagonist antibodies directed towards VEGFR1 (**F**) or VEGFR2 (**G**) both at 25 μg/ml, and incubation was continued in their presence throughout the assay. NT indicates non-treated controls. All results are expressed as Average ± SD. Statistical comparisons to NT are indicated by: *** for $P < 0.001$, ** for $P < 0.01$, * for $P < 0.05$; in (E), # indicates $P < 0.05$ compared to R1.

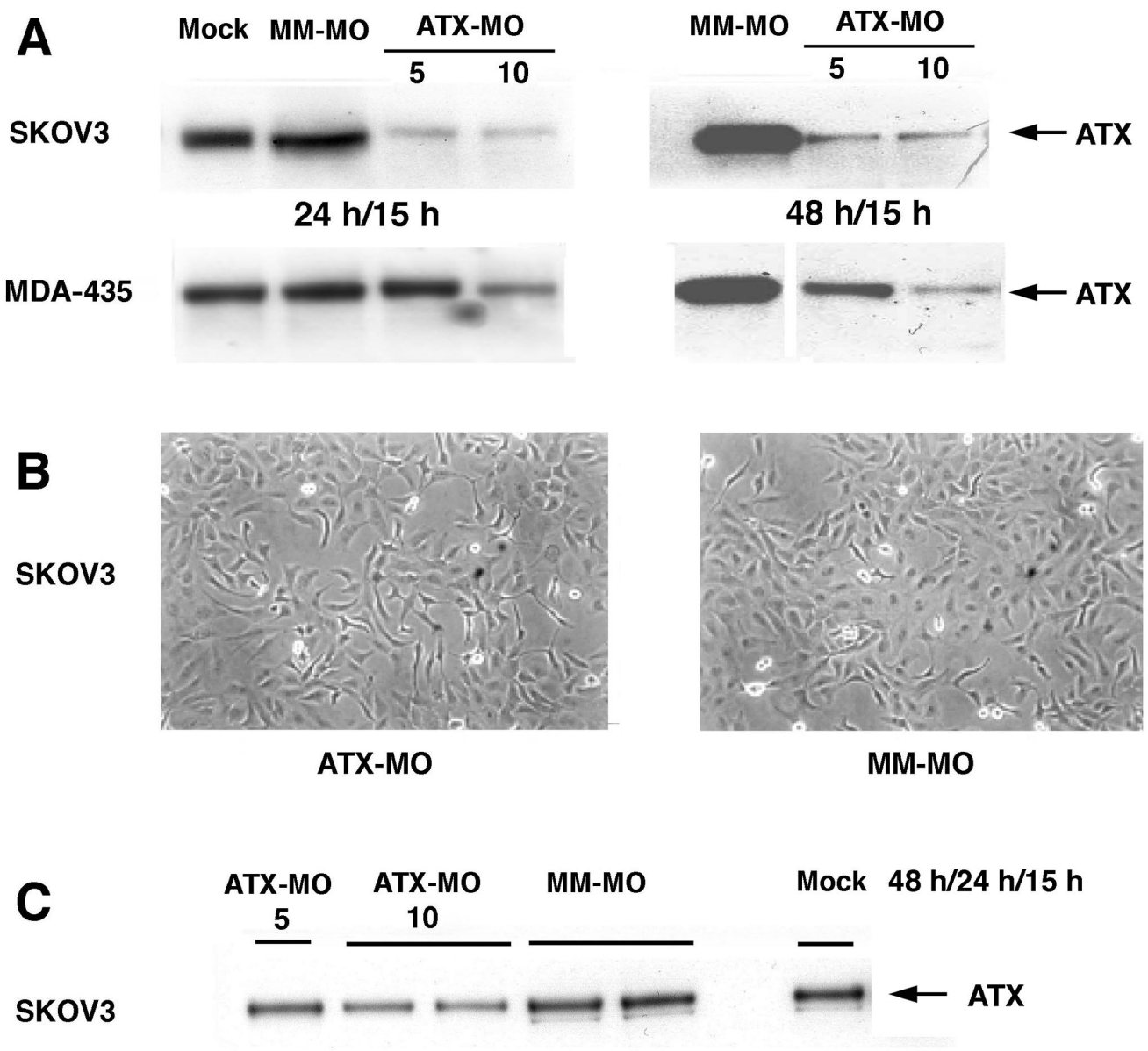

Figure 4. Transient reduction of ATX expression in SKOV3 cells utilizing morpholino oligomers

SKOV3 and MDA-MB-435 (MDA-435) cells were treated with ATX-specific MO oligomers (ATX-MO), mismatched MO oligomers (MM-MO), or Endo-Porter transfection reagent alone (Mock) for 24 h or 48 h, then washed and incubated without morpholinos (indicated as MO incubation time/washout time). The last 15 h of incubation without morpholinos were carried out in serum-free medium. (**A**) ATX immunoblot analysis of treated cells after 24 (left side) and 48 h (right side). (**B**) Phase-contrast light microscopy (100X) of SKOV3 cells after 48h treatment ATX-MO *vs*. MM-MO (both at 10 μM). (**C**) ATX immunoblot analysis of SKOV3 cell supernatants treated for 48 h, and then allowed to recover for 24 h in serum-containing medium and 15 h in serum-free medium before analysis.

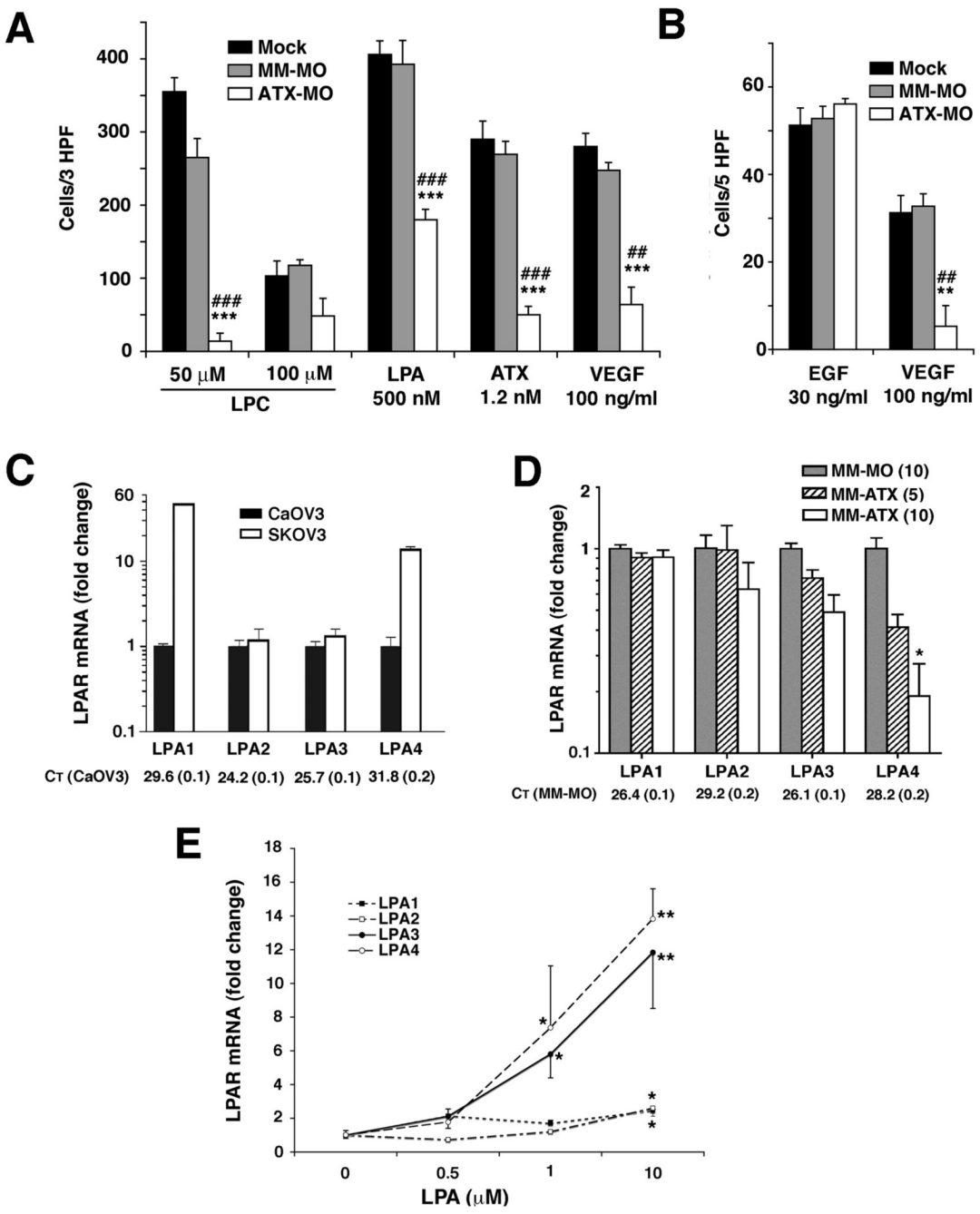

Figure 5. Effects of ATX-MO treatment on cell motility and LPA receptor expression

In (A) and (B) SKOV3 cells were cultured with 10 μM morpholino oligomers that were specific for ATX (ATX-MO) or mis-matched (MM-MO) or with Endo-Porter alone (Mock) for 48 h and then transferred to serum-free medium for an additional 15 h. Chemotaxis assays were incubated for 8h (**A**) or 5h (**B**) utilizing attractants at the indicated concentrations. These results are expressed as Average ± SEM with background motility subtracted out to normalize the data for treatment groups. Statistical comparisons to mock-treated cells are shown as: ***, $P < 0.001$; **, $P < 0.01$; *, $P < 0.05$, and comparisons to MM-MO-treated cells: ###, $P < 0.001$; ##, $P < 0.01$; #, $P < 0.05$. In (C) CaOV3 and SKOV3 cells were cultured under standard conditions and RNA was harvested for quantitative RT-PCR analysis. In (D) SKOV3 cells

were treated with morpholino oligomers as described for (A) and (B) but the intermediate concentration of 5 μM ATX-MO is also shown. RNA was harvested and LPA receptor expression was quantified using RT-PCR. (**E**) LPA receptor expression was quantified after CaOV3 cell treatment at the indicated concentrations of LPA with untreated cells arbitrarily set as 1.0. Results in (**C**), (**D**), and (**E**) are expressed as Average ± SD. In (**D**) statistical comparisons relative to MM-MO are shown as * for $P < 0.05$; in (**E**) statistical comparisons relative to the appropriate untreated LPA receptor are shown as: **, $P < 0.01$ or *, $P < 0.05$.

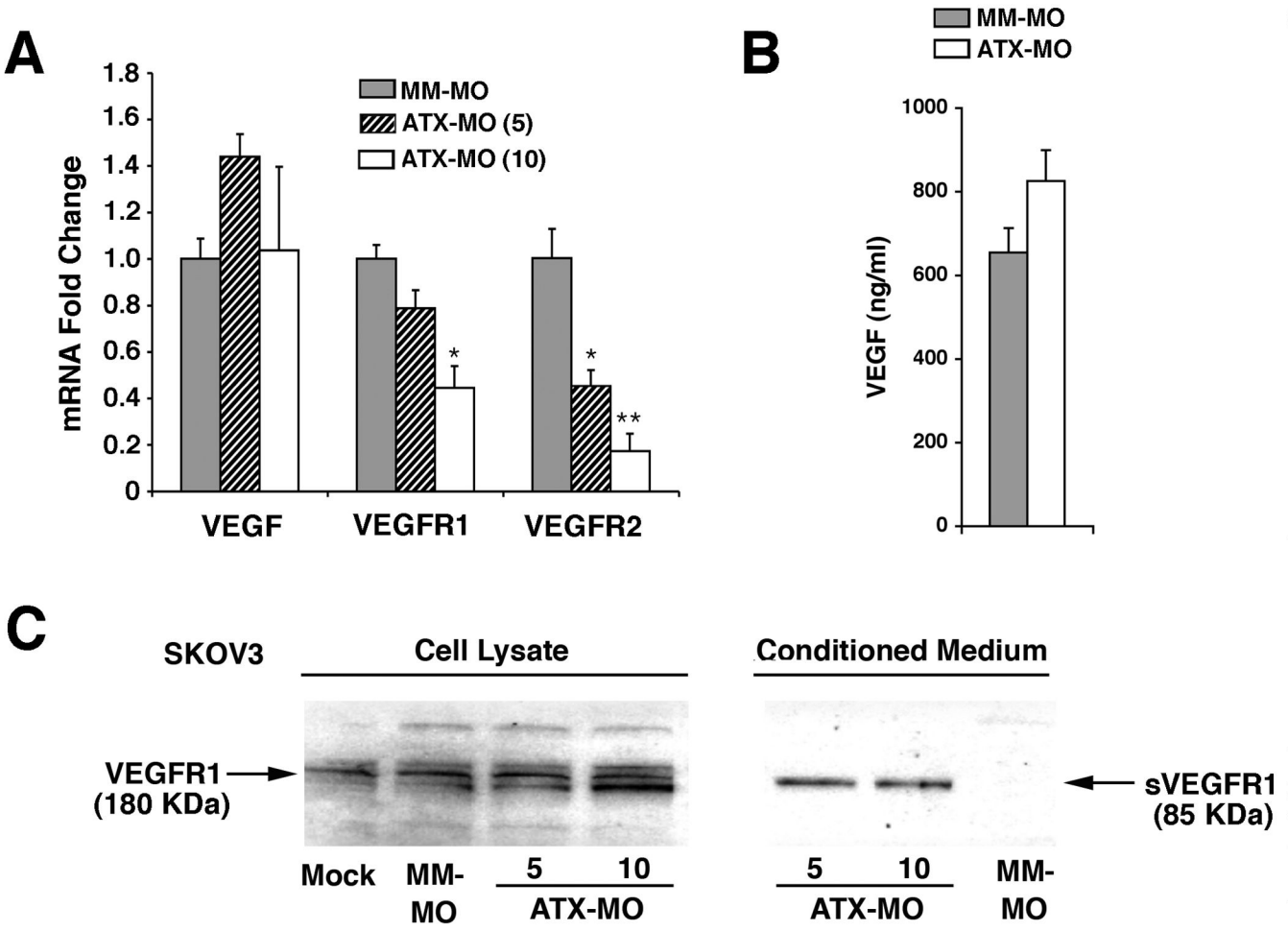

Figure 6. ATX reduction modulates expression of VEGF receptors

(A) Quantitative RT-PCR determination of VEGF, VEGFR1, and VEGFR2 steady-state mRNA levels in SKOV3 cells are shown for ATX-specific knockdown (5 or 10 μM ATX-MO) *vs*. control (10 μM MM-MO). Values were adjusted to TAF9 internal control values and then expressed as fold difference ± S.D. Statistical comparisons relative to the MM-MO treatment group are shown as: **, $P < 0.01$; *, $P < 0.05$. (B) VEGF protein levels measured by ELISA in SKOV3 cell culture supernatants after ATX-MO *vs*. MM-MO treatment. Results are shown as Average ± SD. (C) Immunoblot analysis for VEGFR1 protein in SKOV3 cells treated as indicated from total cell lysates and cell culture supernatants. The truncated, alternatively spliced VEGFR1 product is designated sVEGFR1.

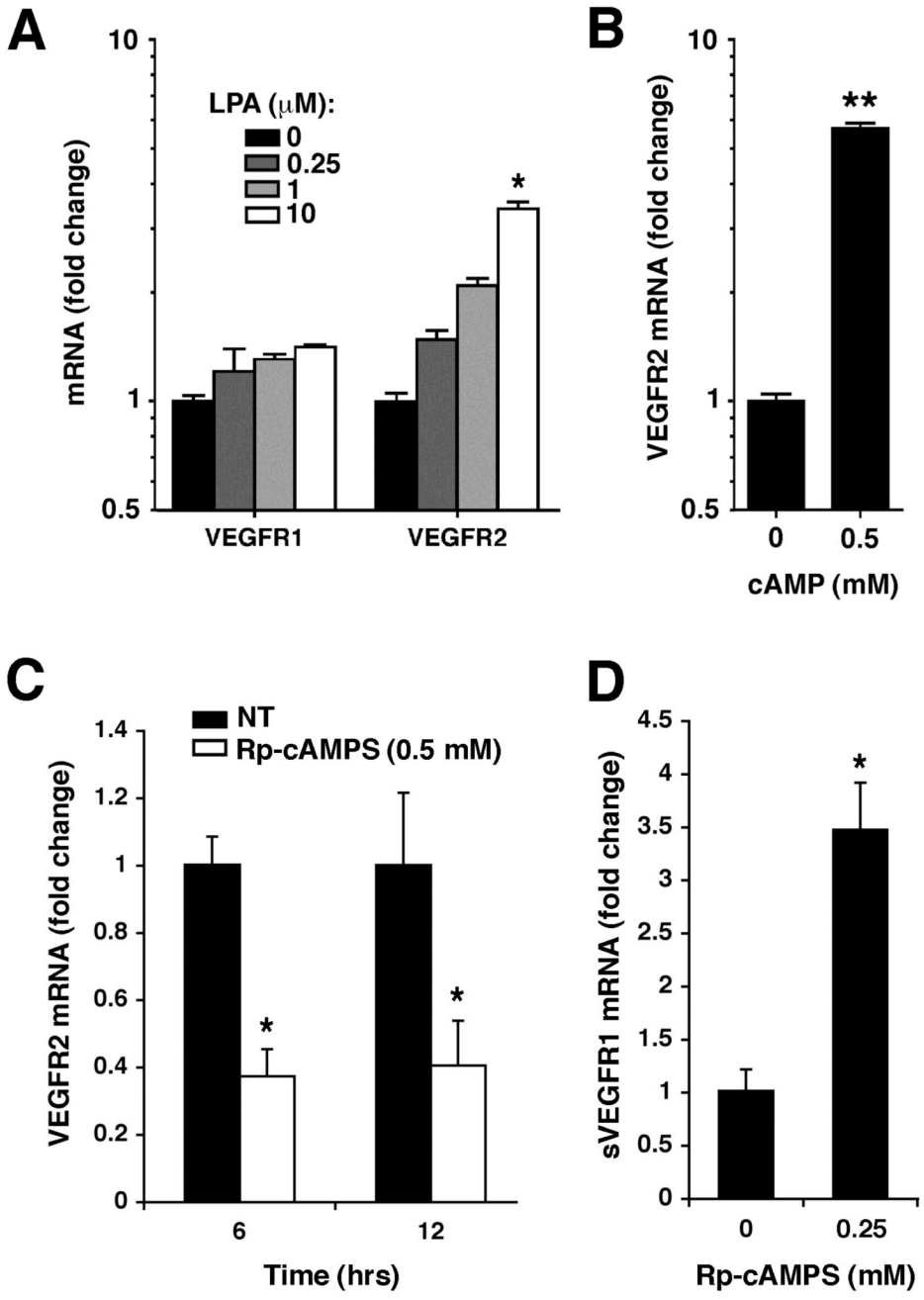

Figure 7. VEGFR expression is induced by LPA and cAMP

(**A**) CaOV3 cells were treated with varying concentrations of exogenous LPA and mRNA levels of VEGFR1 and VEGFR2 were measured by quantitative RT-PCR. In (B–D), SKOV3 cells were incubated in the presence of dibutyryl-cAMP (B) or the PKA inhibitor Rp-cAMPS (C–D) at the indicated concentrations. VEGFR2 expression (B, D) or sVEGFR1 (C) was measured by quantitative RT-PCR. Results are expressed as Average ± SD. Statistical comparisons relative to untreated controls are shown as: **, $P < 0.01$ or *, $P < 0.05$.

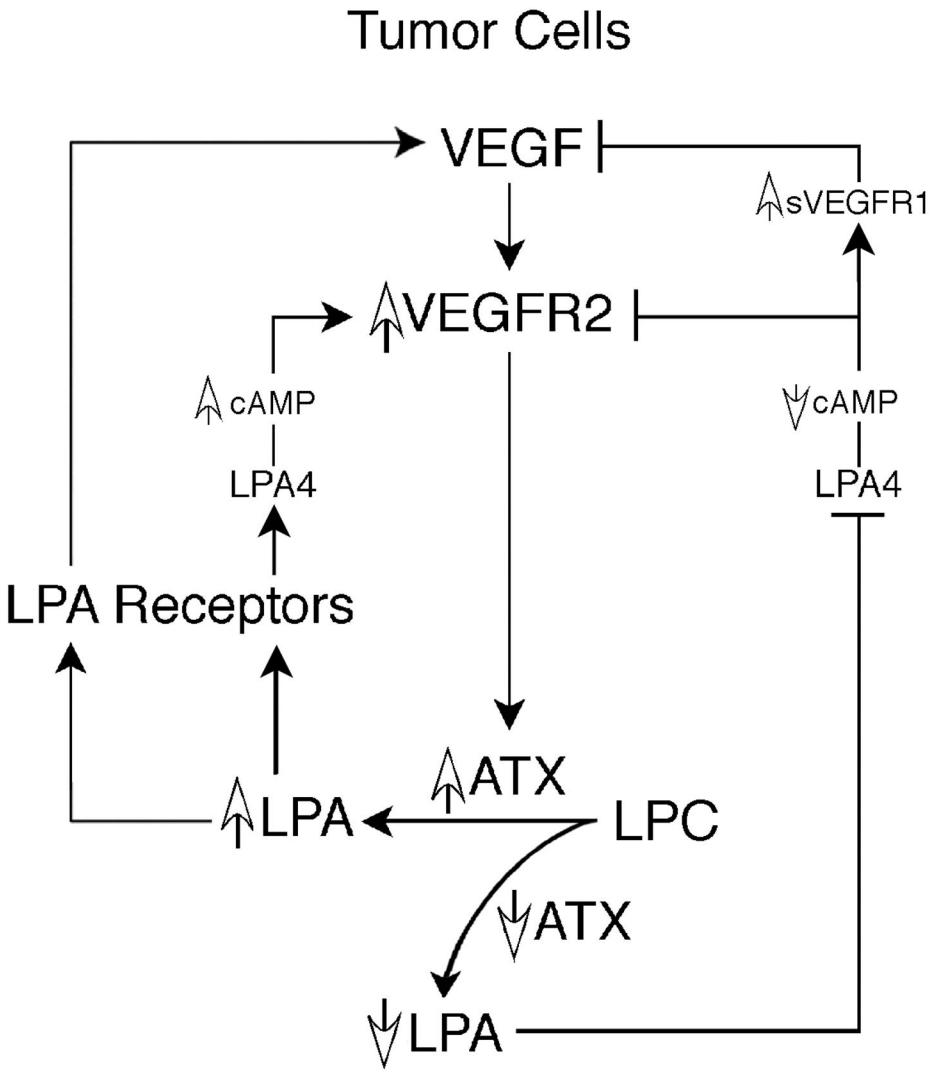

Figure 8. Proposed positive feedback loop between ATX, LPA, and VEGF in ovarian cancer cells

VEGF activates ATX transcription and subsequent protein secretion through VEGFR2. Increased secretion of ATX enables increased extracellular hydrolysis of the ATX substrate LPC, resulting in increased extracellular LPA. Completing the loop, LPA can stimulate VEGF and VEGFR2 expression through LPA receptor signaling. Experimentally, decreasing ATX expression results in decreased extracellular LPA. This reduced availability of LPA results in decreased expression of LPA_4 and thus signaling initiated by this receptor is reduced, particularly activation of adenylyl cyclase. Decreased intracellular cAMP results in decreased VEGFR2 expression and increased expression of the soluble form of the VEGFR1 receptor, sVEGFR1. The net effect of an ATX knockdown is decreased signaling through VEGFR2 and LPA_4.